Nuclear Safety
NEA/CSNI/R(2019)11
November 2022
www.oecd-nea.org

Phase III of the Assessment of Structures Subjected to Concrete Pathologies (ASCET): Final Report

OECD
BETTER POLICIES FOR BETTER LIVES

NEA
NUCLEAR ENERGY AGENCY

Nuclear Energy Agency

NEA/CSNI/R(2019)11

Unclassified English text only

23 November 2022

NUCLEAR ENERGY AGENCY
COMMITTEE ON THE SAFETY OF NUCLEAR INSTALLATIONS

Phase III of the Assessment of Structures Subjected to Concrete Pathologies (ASCET): Final Report

This document is available in PDF format only.

JT03508356

ORGANISATION FOR ECONOMIC CO-OPERATION AND DEVELOPMENT

The OECD is a unique forum where the governments of 38 democracies work together to address the economic, social and environmental challenges of globalisation. The OECD is also at the forefront of efforts to understand and to help governments respond to new developments and concerns, such as corporate governance, the information economy and the challenges of an ageing population. The Organisation provides a setting where governments can compare policy experiences, seek answers to common problems, identify good practice and work to co-ordinate domestic and international policies.

The OECD member countries are: Australia, Austria, Belgium, Canada, Chile, Colombia, Costa Rica, the Czech Republic, Denmark, Estonia, Finland, France, Germany, Greece, Hungary, Iceland, Ireland, Israel, Italy, Japan, Korea, Latvia, Lithuania, Luxembourg, Mexico, the Netherlands, New Zealand, Norway, Poland, Portugal, the Slovak Republic, Slovenia, Spain, Sweden, Switzerland, Türkiye, the United Kingdom and the United States. The European Commission takes part in the work of the OECD.

OECD Publishing disseminates widely the results of the Organisation's statistics gathering and research on economic, social and environmental issues, as well as the conventions, guidelines and standards agreed by its members.

NUCLEAR ENERGY AGENCY

The OECD Nuclear Energy Agency (NEA) was established on 1 February 1958. Current NEA membership consists of 34 countries: Argentina, Australia, Austria, Belgium, Bulgaria, Canada, the Czech Republic, Denmark, Finland, France, Germany, Greece, Hungary, Iceland, Ireland, Italy, Japan, Korea, Luxembourg, Mexico, the Netherlands, Norway, Poland, Portugal, Romania, Russia (suspended), the Slovak Republic, Slovenia, Spain, Sweden, Switzerland, Türkiye, the United Kingdom and the United States. The European Commission and the International Atomic Energy Agency also take part in the work of the Agency.

The mission of the NEA is:

- to assist its member countries in maintaining and further developing, through international co-operation, the scientific, technological and legal bases required for a safe, environmentally sound and economical use of nuclear energy for peaceful purposes;
- to provide authoritative assessments and to forge common understandings on key issues as input to government decisions on nuclear energy policy and to broader OECD analyses in areas such as energy and the sustainable development of low-carbon economies.

Specific areas of competence of the NEA include the safety and regulation of nuclear activities, radioactive waste management and decommissioning, radiological protection, nuclear science, economic and technical analyses of the nuclear fuel cycle, nuclear law and liability, and public information. The NEA Data Bank provides nuclear data and computer program services for participating countries.

COMMITTEE ON THE SAFETY OF NUCLEAR INSTALLATIONS (CSNI)

The Committee on the Safety of Nuclear Installations (CSNI) addresses Nuclear Energy Agency (NEA) programmes and activities that support maintaining and advancing the scientific and technical knowledge base of the safety of nuclear installations.

The Committee constitutes a forum for the exchange of technical information and for collaboration between organisations, which can contribute, from their respective backgrounds in research, development and engineering, to its activities. It has regard to the exchange of information between member countries and safety R&D programmes of various sizes in order to keep all member countries involved in and abreast of developments in technical safety matters.

The Committee reviews the state of knowledge on important topics of nuclear safety science and techniques and of safety assessments, and ensures that operating experience is appropriately accounted for in its activities. It initiates and conducts programmes identified by these reviews and assessments in order to confirm safety, overcome discrepancies, develop improvements and reach consensus on technical issues of common interest. It promotes the co-ordination of work in different member countries that serve to maintain and enhance competence in nuclear safety matters, including the establishment of joint undertakings (e.g. joint research and data projects), and assists in the feedback of the results to participating organisations. The Committee ensures that valuable end-products of the technical reviews and analyses are provided to members in a timely manner, and made publicly available when appropriate, to support broader nuclear safety.

The Committee focuses primarily on the safety aspects of existing power reactors, other nuclear installations and new power reactors; it also considers the safety implications of scientific and technical developments of future reactor technologies and designs. Further, the scope for the Committee includes human and organisational research activities and technical developments that affect nuclear safety.

Acknowledgements

Gratitude is expressed to Mr Neb Orbovic for his great effort in implementing and managing the Assessment of Structures Subjected to Concrete Pathologies (ASCET) programme and for managing the workshops with the support of Mr Olli Nevander and Dr Diego Escrig Forano from the Nuclear Energy Agency.

Table of contents

List of figures

List of abbreviations and acronyms

AAR	Alkali aggregate reaction
ASCET	Assessment of Structures Subjected to Concrete Pathologies (NEA)
ASR	Alkali–silica reaction
CAPS	CSNI activity proposal sheet
CG	Centre of gravity
CNSC	Canadian Nuclear Safety Commission
CSNI	Committee on the Safety of Nuclear Installations (NEA)
EDF	Électricité de France
EPRI	Electricity Power Research Institute (United States)
ESSI	Earthquakes, and/or Soils, and/or Structures and their Interaction
FE	Finite element
FEA	Finite element analysis
IAEA	International Atomic Energy Agency
IRSN	Institut Radioprotection Sûreté Nucléaire (France)
LVDT	Linear variable differential transformer
NEA	Nuclear Energy Agency
NIST	National Institute of Standards and Technology (United States)
NRA	Nuclear Regulation Authority (Japan)
NRC	Nuclear Regulatory Commission (United States)
OECD	Organisation for Economic Co-operation and Development
RBSM	Rigid-Body-Spring Model
REF	Re-closure characteristic stress
WGIAGE	Working Group on Integrity and Ageing of Components and Structures (NEA)

Executive summary

The Assessment of Structures Subjected to Concrete Pathologies (ASCET) programme is part of the Working Group on Integrity and Ageing of Components and Structures (WGIAGE) of the Nuclear Energy Agency's (NEA) Committee on the Safety of Nuclear Installations (CSNI). The objective of its activities (Phases I, II and III) is to make general recommendations for ageing management of concrete nuclear facilities, taking into account the effect of concrete pathologies on structural degradation. Concrete pathologies and degradation mechanisms (e.g. alkali aggregate reaction, delayed ettringite formation, irradiated concrete, sulfate attack, reinforcing steel corrosion, freezing and thawing cycles) have been detected in concrete nuclear facilities in several NEA member states and they are likely to affect the performance and the residual lifetime of the nuclear power plants. The ASCET Phase I recognised the need to concentrate on alkali aggregate reaction, provide more test results of reduced and full-scale models, make validations of analysis models and tools and quantify uncertainties in the analysis.

In the ASCET Phase II, blind simulation benchmark participants predicted the behaviour of structural elements with alkali aggregate reaction (AAR), e.g. concrete swelling. The input test data for the ASCET simulations were provided by the Canadian Nuclear Safety Commission (CNSC) research programme with the University of Toronto, where five walls with AAR were tested. The main conclusions of the test campaign are:

- The walls with alkali aggregate reaction have the same or even slightly higher ultimate shear capacity compared to the walls made of regular concrete, despite reduced compressive and tensile concrete strengths. Therefore, the code equations for the design of concrete elements based on concrete compressive strength are not applicable.
- The behaviour of the regular walls did not change significantly with time.
- The walls with alkali aggregate reaction experience, with time, significant loss of ductility and energy absorption, and the hysteresis loops become very narrow.

In the ASCET Phase III, the goal was to assess and develop the Phase II (blind benchmark) recommendations using additional test results. The Phase III simulations were performed using a full set of the test results to calibrate numerical models, perform sensitivity studies and find governing parameters. In the ASCET Phase III benchmark, almost all participants, independently of the software used, calculated peak strength of the walls' capacity to within a 10% difference of the measured values. However, similarly to the Phase II benchmark, the displacements and the shape of the hysteresis loops were more difficult to simulate.

Based on the ASCET work in the three phases, the following recommendations are made:

- In the case of concrete with pathologies/degradation mechanisms, the strength predictions based on the design equations in the current codes do not agree with the results of structural element testing. Therefore, numerical models of design codes need to be validated by using adequate structural test results. In many cases the tests on reduced scale structures cannot provide the correct information related to the performance of full-scale structures in normal conditions. Thus, it is necessary to test both reduced and full-scale models. In addition, there is a need for model validation and quantification of uncertainties in the input data and results.

- There is a need for international expert work to provide acceptance criteria for the design and assessment of concrete structures with alkali aggregate reaction (or any other degradation mechanism resulting in concrete swelling).
- The code equations related to the design capacity of concrete elements which are based on concrete compressive strength are not applicable. Based on the results, the capacity is not directly correlated to the allowable displacements and drifts, as suggested in design standards. Therefore, there is a need to provide separate, uncorrelated sets of acceptance criteria in terms of capacity and deformations.
- The deformation limits are governing and that should be taken into account in the assessment phase.
- New damping values for reinforced concrete elements with alkali aggregates reaction (or any other concrete degradation resulting in concrete swelling) should be provided. The damping values in current design and assessment standards are high compared to the tests and results in underestimation of structural demand for structures with concrete degradation resulting in concrete swelling. Suitable dynamic tests are needed to quantify the structural damping values, and it is important to recognise the sensitivity of results to the material characteristics when analysing and recording the test results.
- The loss of ductility and energy absorption (hysteretic damping) of walls with alkali–silica reaction (ASR) concrete, compared to walls with regular concrete, is an important finding of the test campaign performed at the University of Toronto. The ASCET programme found that the losses of ductility and energy absorption are difficult to model. Special attention should be paid in the assessment of concrete structures with ASR (or any other degradation mechanism resulting in concrete swelling) regarding the simulation of those phenomena and corresponding acceptance criteria.

1. Introduction

The objective of the programme Assessment of Structures Subjected to Concrete Pathologies (ASCET) is to make general recommendations for ageing management of concrete nuclear facilities taking into account the effect of concrete pathologies on structural degradation. The ASCET Phase I workshop was held at the National Institute of Standards and Technology (NIST), Gaithersburg, Maryland (United States), from 29 June to 1 July 2015, and the Phase I report (NEA, 2017) includes the presentations, conclusions and recommendations of the workshop. Based on these recommendations, Phase II was defined as a blind simulation benchmark to predict the behaviour of structural elements with alkali aggregate reaction (AAR), which has as a consequence concrete swelling.

The input test data for the ASCET Phase II simulations was from the Canadian Nuclear Safety Committee (CNSC) research programme with the University of Toronto. The programme was put in place in 2012 to study the behaviour of the structural elements with AAR. Five squat shear walls in total were manufactured, cured and tested at the University of Toronto laboratory under this research programme. Two shear walls (REG A and REG B) were manufactured using regular concrete, and were tested after 240 and 975 days of accelerated ageing (50 degrees C and 95% of humidity). Three walls (ASR A1, ASR B1 and ASR B2) with alkali–silica reactive concrete (a form of alkali aggregate reaction) were tested after 260, 610 and 995 days of accelerated ageing. The walls were tested under cyclic loading.

The test results of two shear walls, REG A (240 days of accelerated ageing) and ASR A1 (260 days of accelerated ageing), were provided to the participants of ASCET Phase II to calibrate numerical models with of goal of predicting the behaviour of the walls REG B (975 days of accelerated ageing) and ASR B2 (995 days of accelerated ageing). The ASR expansions for controlling concrete specimens (prisms) aged for the same length of time as the walls were: 0.19% (ASR A1), 0.215% (ASR B1) and 0.223% (ASR B2).

2. Test set-up

A schematic view of the shear wall test set-up is shown in Figure 2.1. The lower beam is fixed on the strong floor with a steel beam and the strong anchor in its centre and laterally, with the two inch steel plates (details of lateral support can be seen in Figure 2.2). The upper beam is free to rotate during the lateral cyclic loading. A dead load of 800 kN was applied on the upper beam. Figure 2.2 a) shows loading cycles and their number as well as the position of linear variable differential transformer (LVDT) gauges for lateral displacement measurements. The measured displacements provided to the participants were the displacements of the A-frame (the difference between the top displacements and two bottom displacements).

Figure 2.1. Schematic of the test set-up

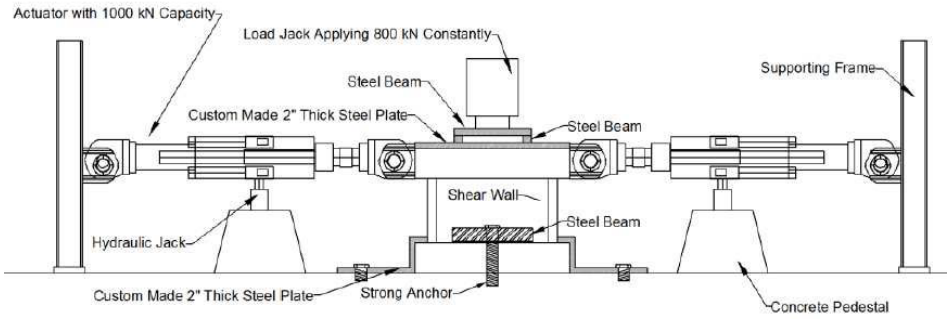

Source: NEA, 2019.

Figure 2.2. Number of cycles and placement of gauges

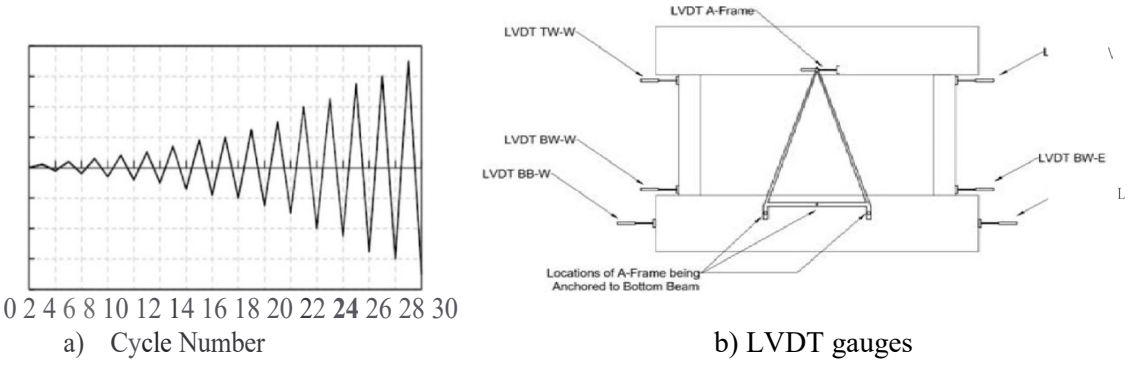

Source: NEA, 2019.

3. ASCET Phase II workshop recommendations

The ASCET Phase II workshop was held at the Canadian Nuclear Safety Commission (CNSC) headquarters in Ottawa on 8-9 May 2017. The participants presented the results of blind simulations. These results were mainly focused on the ultimate wall capacity, which was predicted successfully by participants.

Boundary conditions were one of the main topics of discussions during the ASCET Phase II workshop. Their influence on the results, especially on wall displacements, was judged by the participants to be more important than the influence of concrete constitutive laws.

The loss of ductility over time of alkali–silica reaction (ASR), manifested with pinched hysteresis loops and decreasing strain energy, is another important point, especially for seismic loading, and should be studied in detail.

The recommendation of the workshop was to perform another round of simulations, ASCET Phase III, focused on prediction and evaluation methods related to output results such as:

- displacements;
- deformations;
- the failure modes;
- the crack pattern, crack width and crack distribution.

These parameters are quite important from the viewpoint of the usability of simulation tools, since they significantly affect the serviceability of concrete structures. To study these parameters, additional test data were needed.

4. Additional test data provided by the University of Toronto

To address the recommendations of the ASCET Phase II workshop, there was a need for additional test data from the University of Toronto, especially related to boundary conditions, displacement measurements, the condition of walls prior to and during testing and the test protocol, with available photos, videos and measurements.

The test results of all five walls, including the intermediate ASR B1 (610 days of curing), were provided to the participants.

Based on the discussion during the ASCET Phase II workshop, the University of Toronto provided the following additional data:

- Details regarding boundary conditions: connection of the wall to the strong floor.
- Pictures of walls before and during the tests with measured crack width.
- Excel sheets with force-displacement curves for all five wall tests (REG A, REG B, ASR A1, ASR B1 and ASR B2). The sheets include the intermediate ASR B1 (610 days of curing).

As shown in Figure 4.1, the shear wall was laterally constrained on both ends of the bottom concrete beam to prevent any slippage, by using a 50 mm thick steel plate (150 mm x 300 mm) and a 50.8 mm post-tensioned bolt. These bolts were connected to the columns, which were anchored to the strong floor on each side of the wall (Figure 4.1 (b)). In addition, the shear wall specimens were anchored to the strong floor (Figure 4.1 (c)). A constant axial load of 800 KN was applied and maintained throughout the test on the top surface of the top concrete beam (Figure 4.1 (c)).

Figure 4.1. Experimental set-up of shear wall specimens.

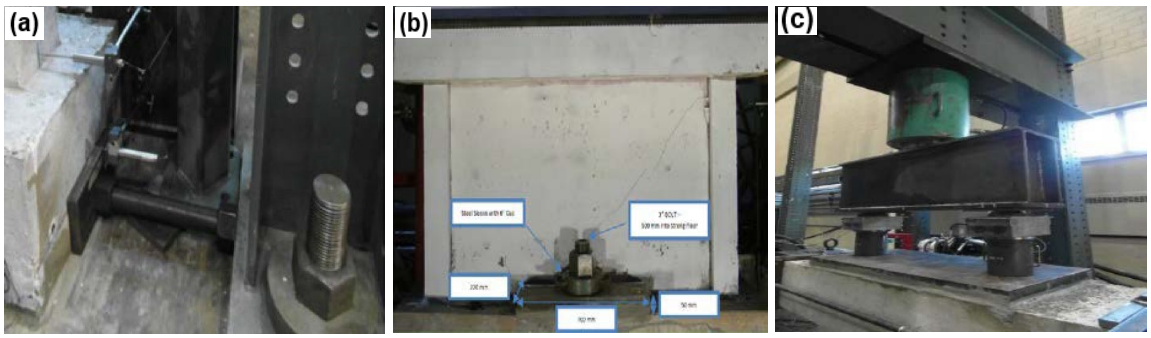

Source: Univeristy of Toronto, 2022.

Data on the crack pattern and crack width during different levels of horizontal force were also requested from the University of Toronto. On Figure 4.2, the crack pattern is shown for different levels of horizontal forces for wall ASR B1. Diagonal shear cracks developed at a low level of loading and developed further up to the failure. Force-displacement curves for regular and alkali aggregate reaction (AAR) walls are presented in Figure 4.3 and Figure 4.4. Regular walls show similar behaviour despite different ages (240 and 975 days). The shapes of the hysteresis loops are very similar as well as the maximum shear force and

maximum displacement. The hysteresis loops show two slopes with decreasing tangent angle with increasing loading.

Figure 4.2. Crack pattern in the wall ASR B1 for different levels of horizontal forces

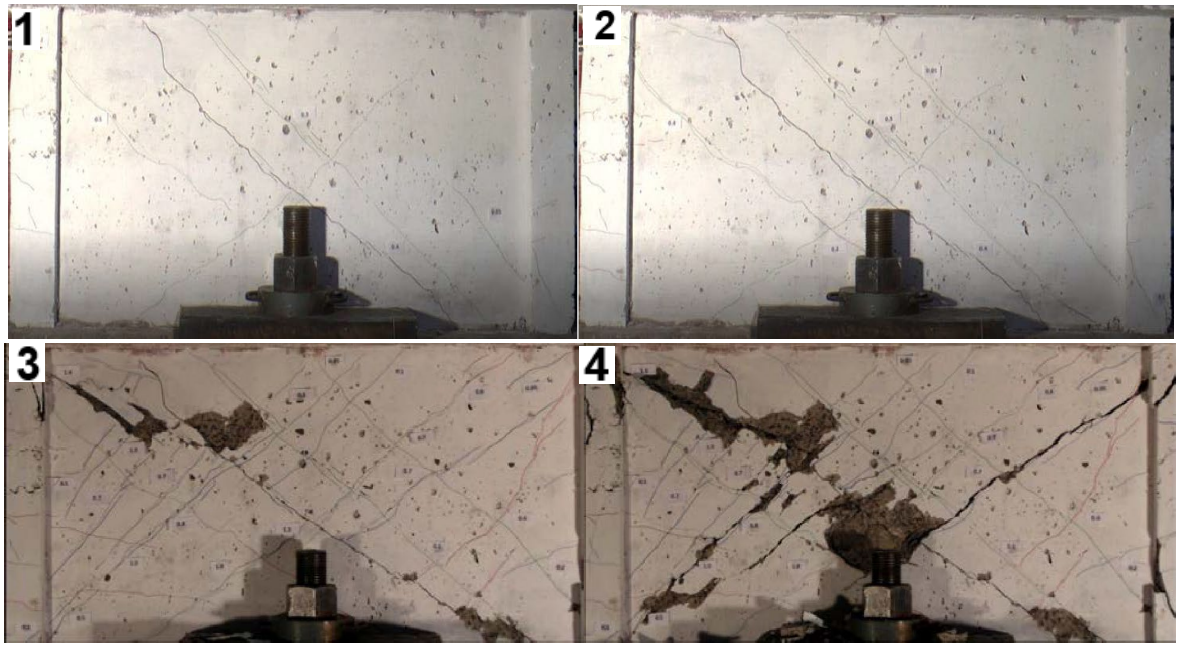

Source: Univeristy of Toronto, 2022.

Force-displacement functions for walls with AAR show a big difference in wall behaviour between the ASR A1 wall on one side and ASR B1 and ASR B2 walls on the other side. Hysteresis loops are much wider and displacements are larger in ASR A1 than in ASR B1 and ASR B2 walls for an unknown reason. For the ASR B1 and ASR B2 walls, the trend is for very narrow hysteresis loops and very low displacements. Hysteresis loops in ASR A1 wall are wider than in regular walls. The results of ASR A1 wall should not be used for any general conlusion or recommendation. However, the results are presented for information.

Figure 4.3. Force-displacement curves for regular concrete walls REG A (240 days) and REG B (970 days)

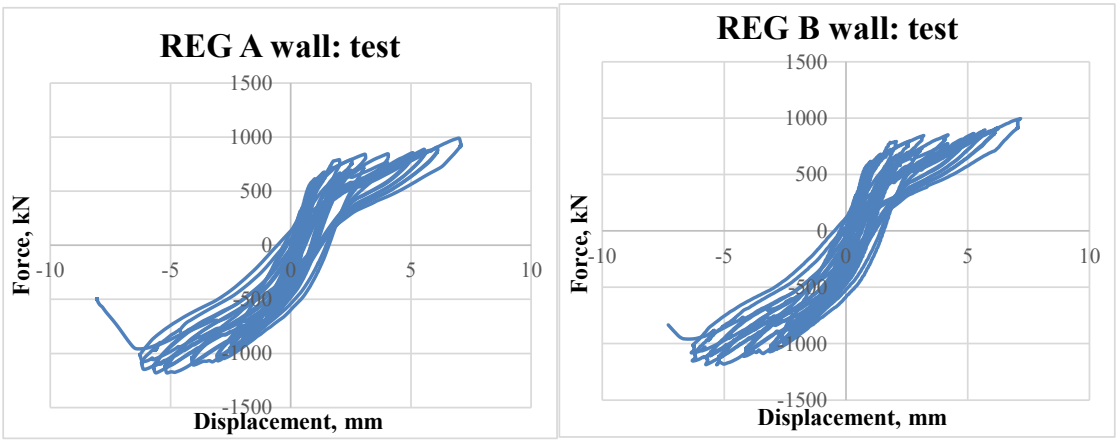

Figure 4.4. Force-displacement curves for walls with alkali aggregate reaction ASR A1, and ASR B1, ASR B2

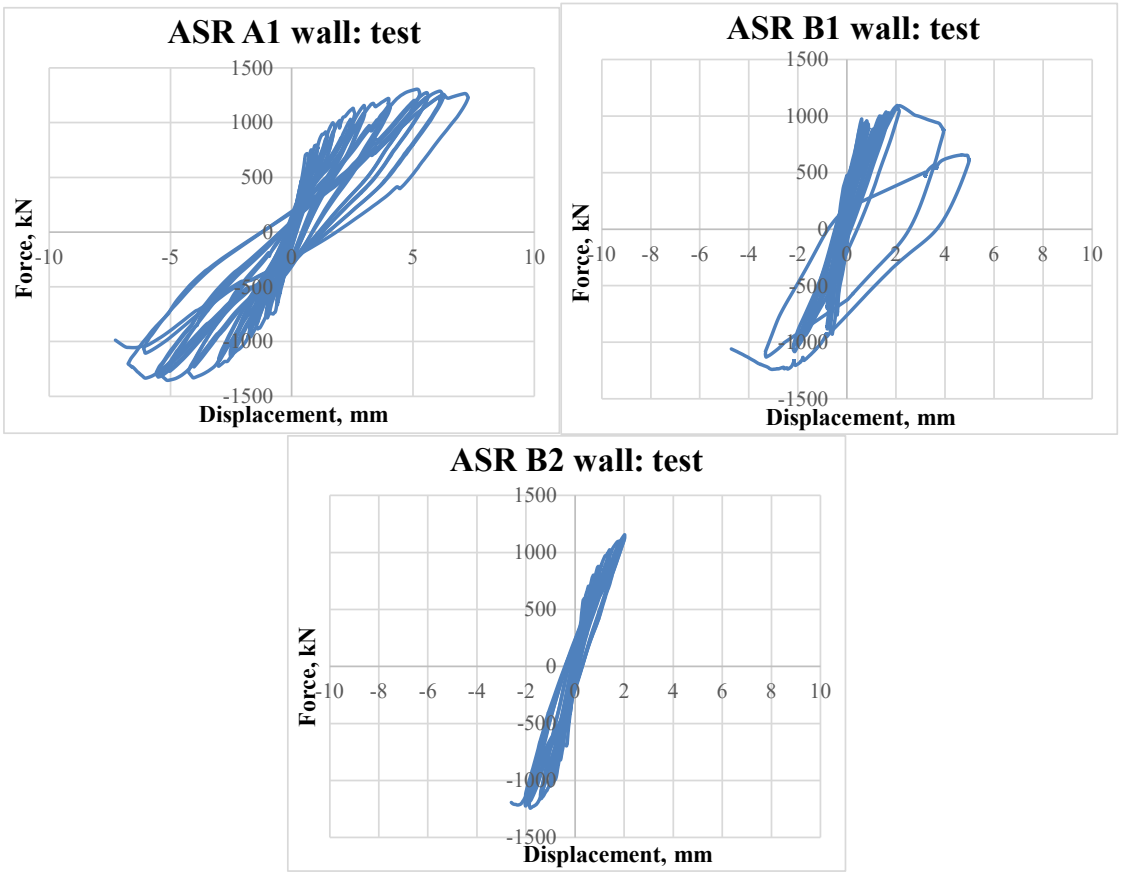

Source: NEA, 2019.

Additional information related to the loading protocol was provided based on the CNSC analysis and questions to the University of Toronto. The cyclic loading was applied up to a certain point, close to the rupture of the wall. From that point, the test was performed under the horizontal loading in one direction and reduced axial force. For this reason, the simulations of the last cycles, and at the failure of the wall, should be taken with caution.

5. ASCET Phase III workshop

The ASCET Phase III workshop was held at the NEA Headquarters in Boulogne, France, on 16-17 April 2018. The goal of the workshop was to address the Phase II recommendations using additional test results. The Phase III simulations were performed using a full set of test results in order to calibrate numerical models, perform sensitivity studies and find governing parameters.

6. Summary of the Phase III results

6.1 US NRC report

The software programmes used in the US NRC study for 2D and 3D non-linear finite element analysis were VecTor3 and VecTor2 developed by the University of Toronto (Wong, Vecchio and Trommels, 2002). VecTor2 (2D non-linear analysis) uses a plane stress formulation with features to account for, in approximation, out-of-plane concrete expansion and resulting confinement provided by out-of-plane reinforcement. These features make it possible to consider the confinement provided by the stir-ups in the end elements (columns) of the shear walls. Two 3D models were developed in which the reinforcement was modelled in two different ways, i.e. smeared reinforcement and discrete reinforcement; brick solid elements are used to model the concrete.

The boundary conditions are as follows: the vertical displacements at the bottom of the concrete beam and the horizontal displacement at the centre of gravity (CG) of the bottom concrete beam are fixed.

Based on a comparison of the results of 2D, 3D smeared and 3D discrete reinforcement, the 3D discrete reinforcement model was selected for this benchmark and sensitivity studies.

Figure 6.1. US NRC baseline: Force-displacement curves comparison test- analysis results for regular concrete walls RAG A and REG B (red circles represent the peak shear force)

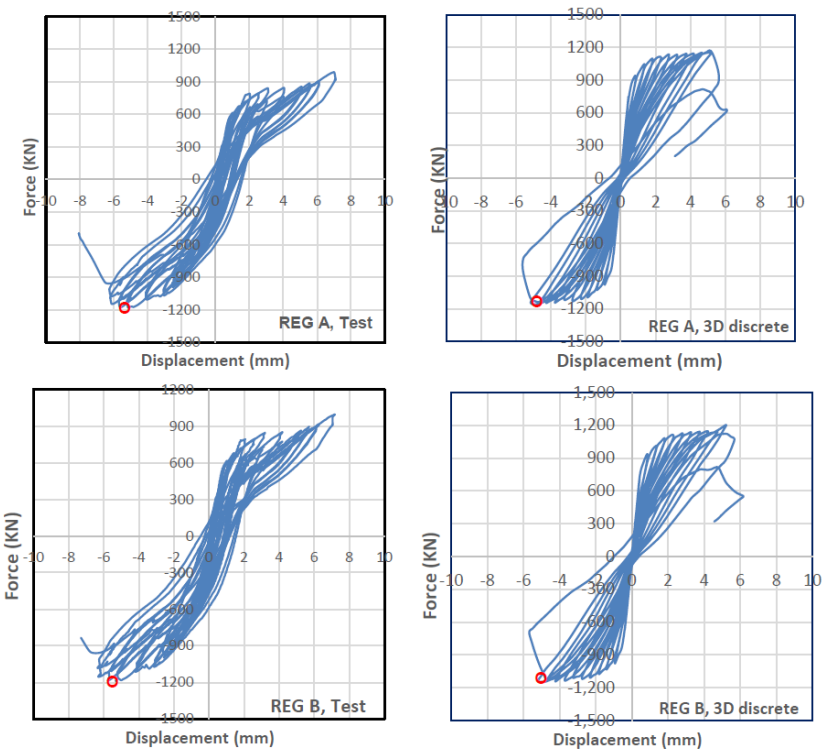

Source: NEA, 2019.

The results of the US NRC baseline study using a 3D discrete model are presented in Figure 6.1 (regular walls) and Figure 6.2 (walls with alkali aggregate reaction). For the regular walls, the maximum capacity is well predicated; however, the displacements are underestimated and the model does not reproduce the two-slope hysteresis curves. For the walls with alkali aggregate reaction (ASR B1 and ASR B2), the peak strength is captured well but in these cases the models overestimate the displacements of walls with ASR. The pictures of the crack pattern and the failure modes show relatively good agreement with the test results as can be seen in Figure 6.3 (ASR expansion 0.32%). As previously mentioned, the test results of ASR A1 wall should be taken with caution.

Figure 6.2. US NRC baseline: Force-displacement curves comparison test- analysis results for regular concrete walls RAG A and REG B

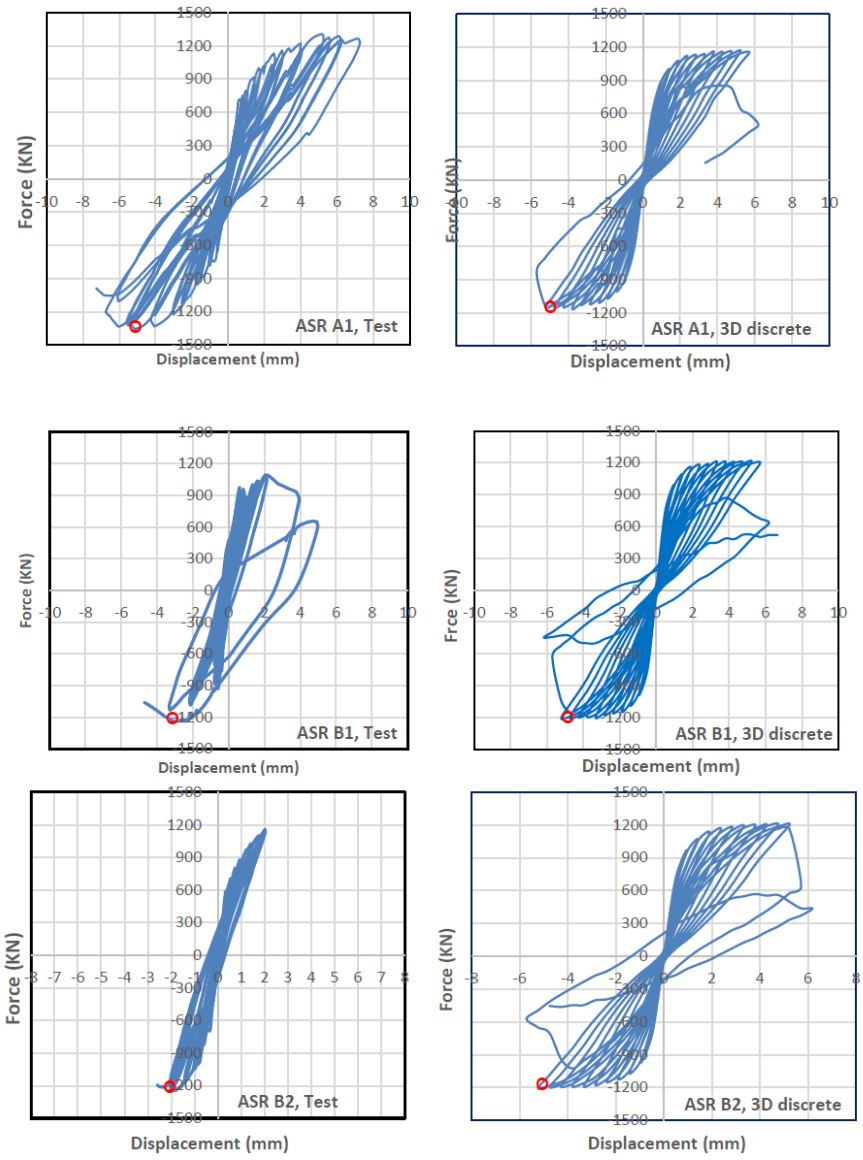

Source: NEA, 2019.

All three simulated failure modes developed an arch from the lower left corner to the lower right corner. This arch simulates the best REG A wall behaviour. The ASR B2 wall has different failure modes with one major diagonal crack from the lower left corner to the upper right corner, without arch effect. To assess the effects of different parameters, the US NRC has performed a series of sensitivity studies.

Figure 6.3. Crack pattern and failure modes REG A, ASR A1 and ASR B2 walls

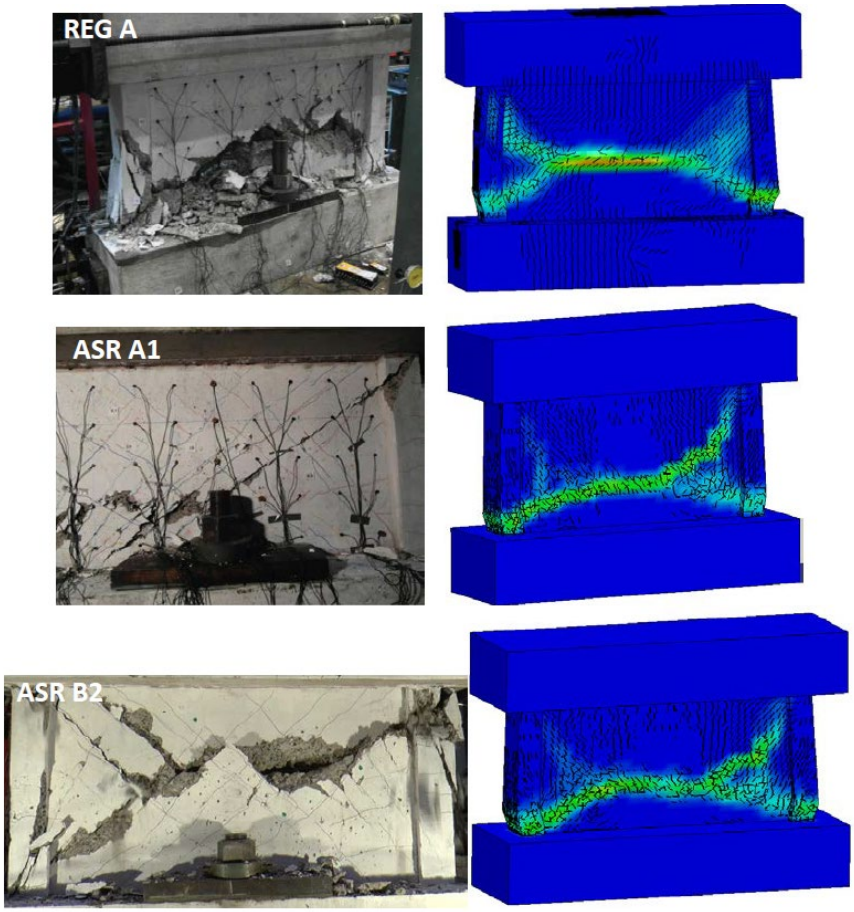

Source: University of Toronto, 2022.

Parametric/Sensitivity studies

The sensitivity studies performed involve the following parameters: 1) effect of concrete expansion on wall capacity 2) effect of maximum aggregates size, and 3) the effect of concrete models.

Effect of concrete expansion

The results of the sensitivity study regarding the concrete expansion due to the alkali aggregate reaction are presented in Figure 6.4. The failure mode changed from the shear failure mode to the shear-friction mode at the connection between the wall and the lower beam. The capacity of the wall was unchanged; however, the displacements and the failure mode were different for expansions 0.32% and 0.35%. This level of expansion is well

above the level of expansion of the controlling specimens (prisms) aged for the same length of time as the walls tested at the University of Toronto (0.223%)

Figure 6.4. Force-displacement curves, crack pattern and failure modes of ASR B1 wall for 0.32% and 0.35% expansion

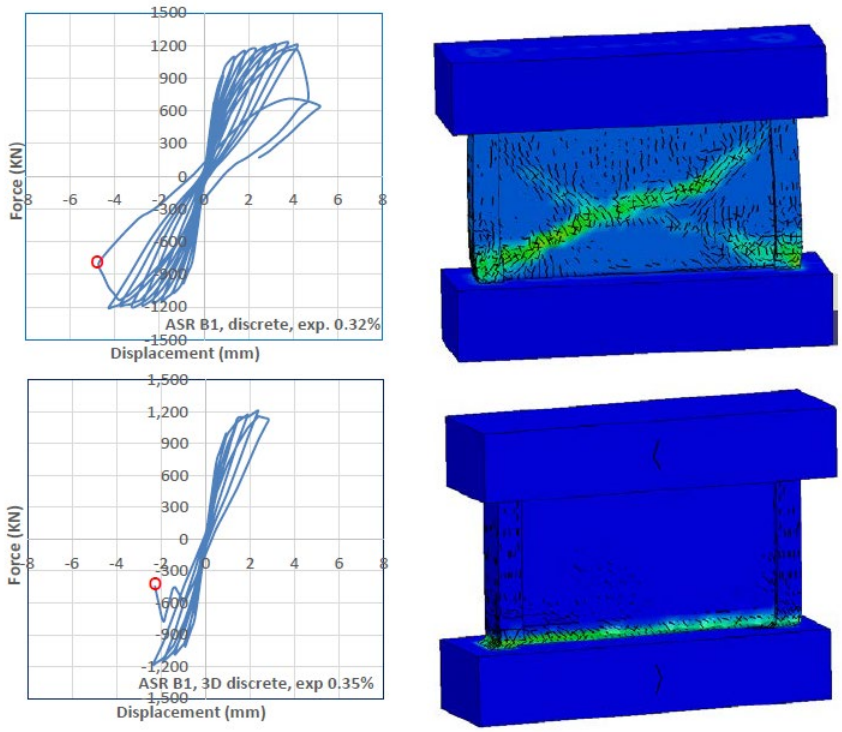

Source: NEA, 2019.

Effect of maximum aggregate size

The US NRC has already addressed the effect of aggregate size during the ASCET Phase II and found that the failure mode is sensitive to the maximum aggregate size. The concrete expansion was kept constant at 0.3% and the maximum aggregate size varied: 10 mm, 12 mm, 15 mm and 20 mm. The change for 20 mm to 15 mm maximum aggregate size has a similar effect as the change from 0.32% expansion to 0.35% expansion shown on Figure 6.4. The failure mode was changed in the same way as shown on Figure 6.4. The maximum shear force is not sensitive to the change of aggregate size. The maximum aggregate size used in the tests was 19 mm.

Effect of concrete expansion models

Three expansion models were used in the sensitivity study: Charlwood et al. 1992, Gautam 2015 and Sellier et al. 2009. The Gautam 2015 and Sellier et al. 2009 models produce different failure (shear-friction at the connection of the wall with the lower beam) than the Charlwood et al. 1992 model with earlier failure at lower displacements. The difference is very similar to the results of two previous sensitivity studies and Figure 6.4. The maximum shear force is still the same, reaching 1 200 kN and the displacements decrease from 5.7 to 2.7 mm.

Effect of concrete model combination

The concrete models deal with three regimes: compression pre-peak (Hoshikuma 1997, Popovics HSC), compression post-peak (Hoshikuma 1997, Montoya 2003) and compression softening (Maekawa 1978, Vecchio 1992-B). Three combinations of these models are addressed in this sensitivity study: case one (Hoshikuma 1997 and Maekawa 1978), case two (Popovics HSC, Hoshikuma 1997 and Maekawa 1978) and case three (Popovics HSC, Montoya 2003 and Vecchio 1992-B). The maximum shear force was similar in all three cases. However, the failure mode and displacement level differ. The failure for case one is a failure with a diagonal crack and cases two and three produced horizontal cracks close to the bottom of the wall. Case three produces less ductile behaviour than cases one and two.

6.2 EDF report

Software and concrete model

The software used in this study was Code Aster with the concrete models FLUA_PORO_BETON and ENDO_PORO_BETON.

Improvements made for the FE model developed in Phase II

The main difference with the model developed in Phase II is in the boundary conditions. In Phase II, the lower beam was fixed to the floor at the point of the central bolt. In Phase III a sensitivity study was performed with:

1. modelled test set-up and
2. fixed lower beam to the slab.

An additional sensitivity study was performed using variation Re-closure Characteristic Stress (REF). The REF is the stress which is necessary to close the crack. Diminution of ductility was obtained for lower REF (change from 10 MPa used in Phase II to five MPa).

As shown in Figure 6.5 and Figure 6.6, despite the modification, the difference between regular and ASR walls in the reduction of ductility and fracture energy was not successfully simulated. The hysteresis curves of regular walls and walls with alkali aggregate reaction are similar in shape and maximum displacements.

Figure 6.5. Force-displacement curves for REG A wall

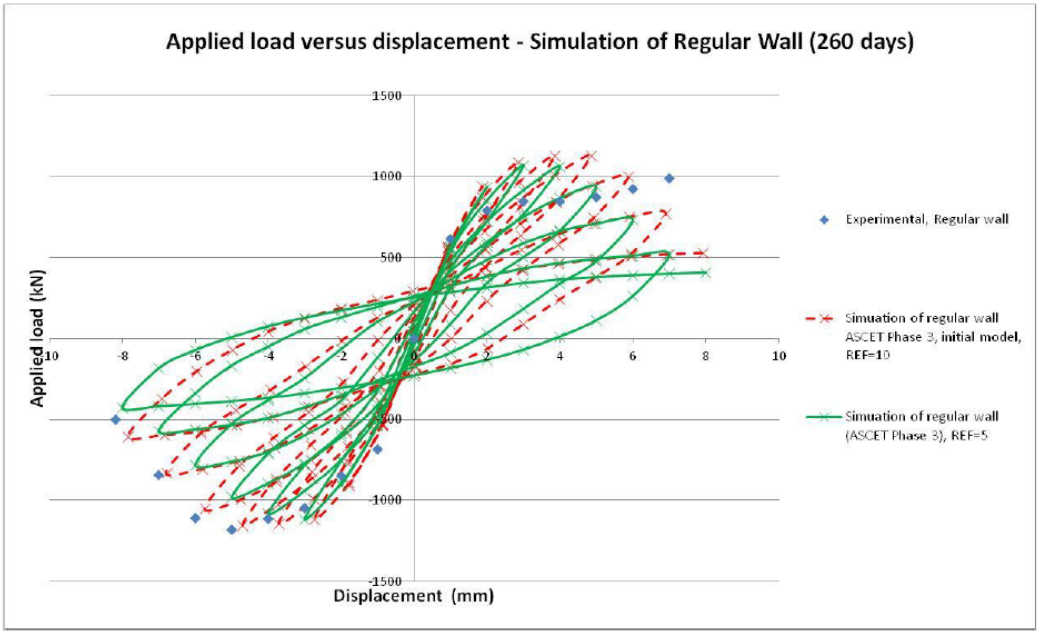

Source: NEA, 2019.

Figure 6.6. Force-displacement curves for ASR B2 wall

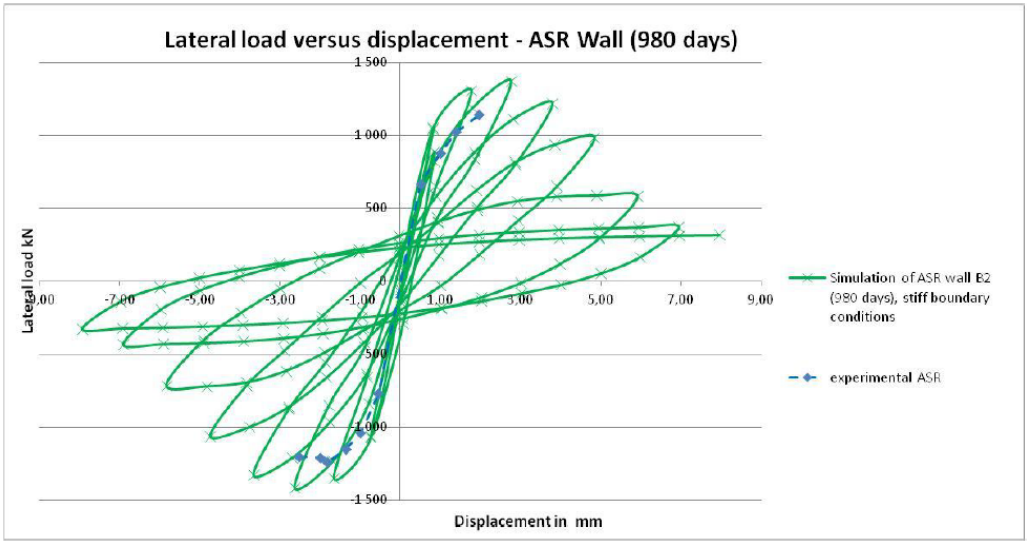

Source: NEA, 2019.

6.3 CNSC report

Software and concrete model

Based on test runs during Phase II, the explicit FE code LS-DYNA, 2-D shell model and non-linear material (concrete) model MAT_172/ *MAT_CONCRETE_EC2 were selected.

Material data and equations governing the behaviour of this model were taken from Eurocode two Part 1.2 (General rules – Structural fire design). The material model could represent plain concrete only, reinforcing steel only, or a smeared combination of concrete and reinforcement. The model includes concrete cracking in tension and crushing in compression, and reinforcement yield, hardening and failure. Properties are thermally sensitive. The concrete expansion due to alkali aggregate reaction was introduced as thermal expansion.

Test data

The CNSC performed a detailed analysis of the data provided by the University of Toronto. Only force-displacement curves of the LVDT A-Frame and total actuator force were provided. Moreover, actuator force and A-frame displacement were not recorded separately as a function of time. The CNSC performed a detailed analysis to understand the wall behaviour.

Based on the CNSC analysis, the questions were posed to the University of Toronto regarding the loading protocol. According to the University of Toronto explanation, lateral load excursions were continued until a significant drop in the axial load was noted in the walls and the walls could not maintain the axial load capacity. From that point forward, the wall was pushed monotonically until failure. The failure point was considered where the wall was no longer capable of taking 40% of applied axial force. However, it is not clear when exactly the switch to monotonic loading was done for each wall and how the axial load was measured.

Improvements made for the FE model developed in Phase II

Following model improvements were implemented in Phase III simulation:

- Absolute value of thermal expansion coefficient αT (equal to longitudinal concrete expansion due to alkali aggregate reaction) was selected instead of relative values.
- Boundary conditions: bottom beam-floor contact and bottom post-tensioned bolts were implemented.
- Upper A-frame displacement was selected as input for constructing force-displacement curves. In ASCET Phase II simulations, actuator prescribed displacements were selected as input, and
- More robust filtering of FE results was applied to mitigate parasitic numerical oscillations caused by employing explicit FE algorithm.

FEA results

The results in terms of force-displacement curves are presented in Figures 6.7 to 6.10. The FEA analysis accurately predicted the ultimate displacement and slightly over predicted the strength of regular walls. The shape of the hysteresis loops was not well predicted, resulting in higher and wider loops and higher energy absorption in FEA. The behaviour of walls B1 and B2 with alkali aggregate reaction was well captured, especially the reduced ductility and narrow hysteresis loops resulting in low energy absorption. It should be noted that the FEA was conducted up to the complete failure of the wall, which was not the case in the tests. This is the explanation for the lower branch of force-displacement curves calculated for the ASR B1 and ASR B2 walls, presented in Figure 6.9 and Figure 6.10.

Figure 6.7. Force-displacement curves for REG A wall: tests and FEA results

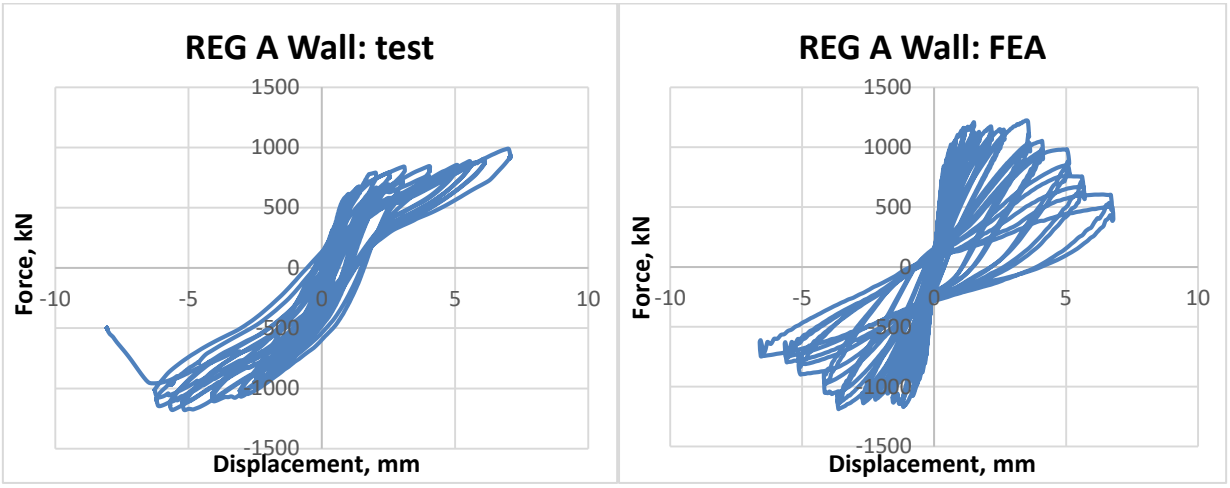

Source: NEA, 2019.

Figure 6.8. Force-displacement curves for REG B wall: test and FEA

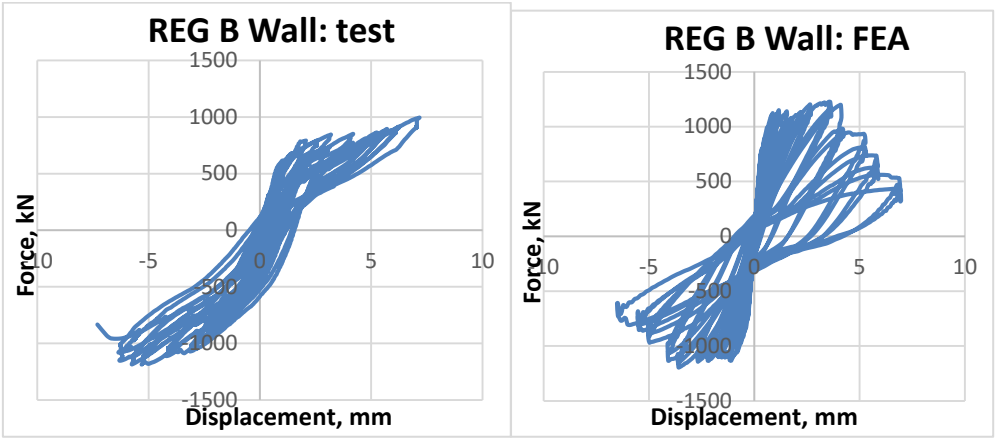

Source: NEA, 2019.

Figure 6.9. Force-displacement curves for ASR B1 wall: test and FEA results

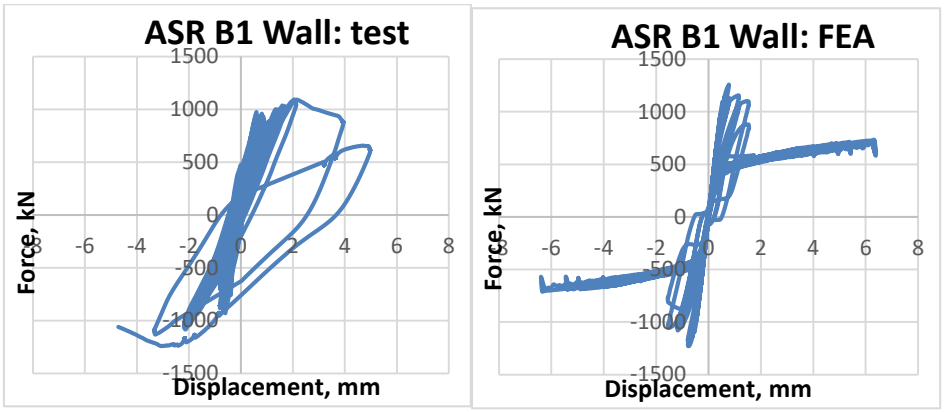

Figure 6.10. Force-displacement curves for ASR B2 wall, test and FEA results

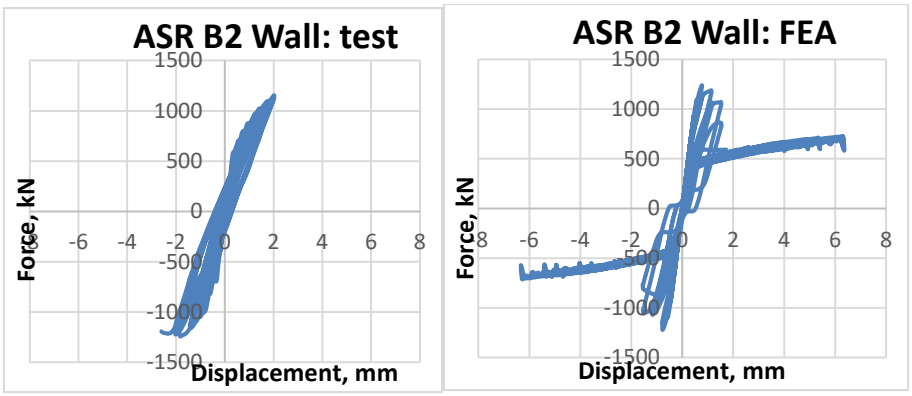

Source: NEA, 2019.

It should be pointed out that the direct comparison between test results and FE predictions for the same number of cycles should be performed with caution because of the following reason: the concrete model employed in FEA assumed no cracks before loading. Therefore, the initial loading cycles produce a much stiffer FE model response without any hysteresis loop (perfect elastic behaviour). Later in the loading, as damage accumulates, both the FE model and the test produce similar responses, see Figure 6.11.

Figure 6.11. Force-displacement curves for the for the 1st and 26th cycle of the REG A wall analysis

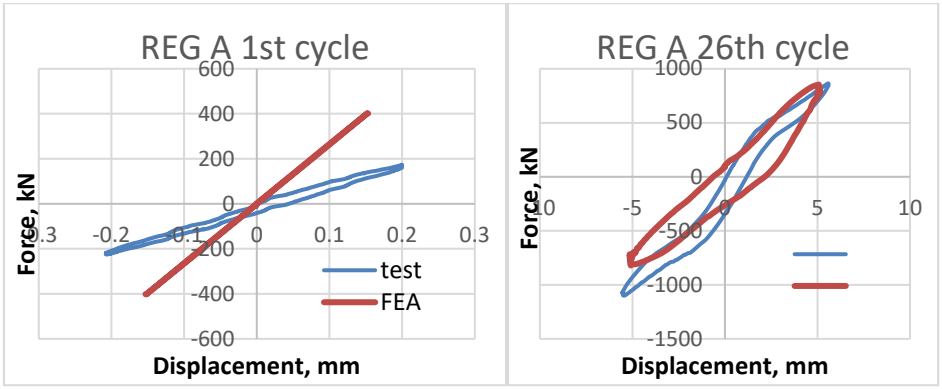

Source: NEA, 2019.

6.4 NRA report

The Nuclear Regulation Authority (NRA) performed the numerical simulations using FINAS/STAR software. Two-dimensional shell and three-dimensional solid elements were used in the analysis. The non-orthogonal three directional smeared crack model of Maekawa and Fukuura was used to introduce a non-linear material model of reinforced concrete to FINAS/STAR. An analytical model of an alkali aggregate expansion from the study of Gocevski's paper (Gocevski, 2016) based on the theory of Pietruszak, which simply expresses the alkali aggregate reaction degradation phenomenon, was incorporated into the non-orthogonal three-directional smeared crack model of the FINAS-STAR.

Boundary conditions

Three cases were studied:

- The lower beam was fixed vertically at the contact with the floor slab and horizontally at the centre of gravity. Sides of the lower beam were fixed horizontally (5-1 Case).
- The lower beam was fixed vertically at the contact with the floor slab and horizontally at the centre of gravity (5-1 A Case).
- Contact elements were placed between the lower beam and the floor slab to enable the lift-up of the lower beam, bottom of anchor bolt was fixed horizontally and the spring was modelled in a vertical direction; the sides of the beam were fixed horizontally (5-2, 5-3 and 5-3 A Case).

The preliminary study has shown that the difference among these boundary conditions were not significant in the behaviour of the wall. The lower beam was affected only with the change of boundary conditions. The analysis was performed with the boundary conditions 1) or as 5-1 Case, without anchor bolts.

Modelling

Two models were used in this analysis: 2D and 3D models. In the 3D model, the wall reinforcement was modelled in the middle of the wall with a continued line of elements. Based on preliminary analysis, it was concluded that the 3D model gave results that were

closer to the tests results and it was decided to use the 3D model in the prediction of the behaviour with alkali aggregate reaction.

Analysis results

The analysis results of the wall with regular concrete and the wall with reactive concrete showed similar behaviour. The hysteresis loops had almost identical shape. Ultimate strength and the maximum displacements were similar. There was no difference in energy consumption between two hysteresis loops. The failure was initiated in both cases by tension at the connection between the wall and the lower beam. The difference between the regular wall and the wall with alkali aggregate reaction was in the width of the compression strut. The compression struts in the wall with alkali aggregate reaction were wider, which can be caused by the lower compression strength of the concrete.

Additional sensitivity studies

A series of additional sensitivity studies was performed varying concrete compression strength, tensile strength, bond characteristic parameters and the possibility of rotation of the upper beam. Seven cases in total were studied. With lower compressive strength, due to alkali aggregate reaction, the peak shear force was reached between 3 mm and 4 mm, which is still above the displacement of 2 mm reached in the experiment. The conclusion made is that the lower compression strength leads to smaller displacements and earlier failure. The other conclusion is that the experiments were affected by the boundary conditions and the material properties of the flange pillar, the loading upper beam and the lower beam.

6.5 University of Toronto report

The software used in the University of Toronto study for 2D and 3D non-linear finite element analysis was VecTor2 software developed by the University of Toronto (Wong, Vecchio and Trommels, 2002). VecTor2 (2D non-linear analysis) uses a plane stress formulation with features to account for, in approximation, out-of-plane concrete expansion and resulting confinement provided by out-of-plane reinforcement. This feature enables consideration of confinement provided by the stirrups in the end elements (columns) of the shear walls.

Sensitivity studies

A series of sensitivity studies included:

- boundary conditions;
- smeared versus discrete reinforcement;
- 3D effect;
- confinement of concrete;
- bond strength;
- reinforcement buckling; and
- cover spalling and element erosion.

The overall conclusion is that three factors were identified as having a notable effect on the computed response: the boundary conditions, strength enhancement due to confinement and concrete compression response (included the post-peak stiffness).

The factors without significant effect are: smeared or discrete representation of the reinforcement, three-dimensional effects, bond strength, reinforcement buckling, cover spalling and element erosion.

However, the sensitivity studies have not shown the main factor for ductility reduction and energy absorption in walls with alkali aggregate reaction.

6.6 Nagoya University report

Modelling

A discrete type numerical model, the Rigid-Body-Spring Model (RBSM) developed by T. Kawai (1978), was used in this analysis. In the RBSM, concrete is modelled as an assemblage of rigid particles interconnected by springs arranged along their interface.

The crack pattern is strongly affected by the mesh design since the cracks initiate and propagate through the interface of particles. Therefore, a random geometry of rigid particles is generated by a Voronoi diagramme, which reduces mesh bias on the initiation and propagation phase of potential cracks. Each rigid particle has three translational and three rotational degrees of freedom defined at the centroid of the particles (Figure 6.12). The interface of two particles is divided into several triangles with a centre of gravity and vertices of the surface as seen in the figure. One normal and two shear springs are set at the centre of each triangle. By distributing the springs in this manner, the model accounts for the effects of bending and torsional moment without any rotational springs (Yamamoto et al., 2008). Figure 6.13. describes constitutive laws used in the model.

Figure 6.12. RBSM and Voronoi diagram

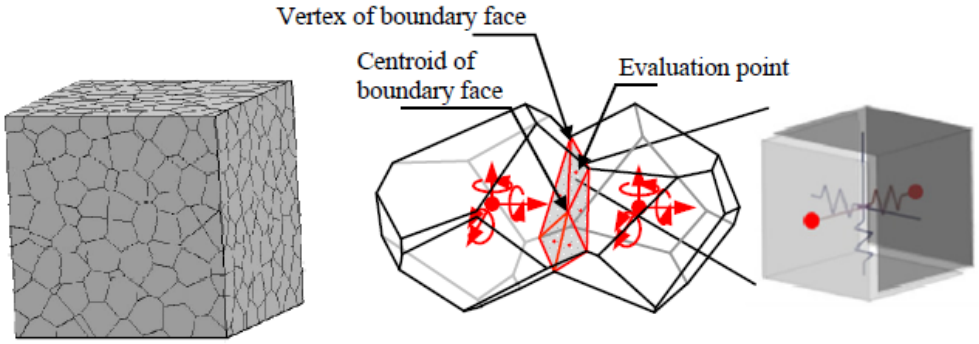

Source: NEA, 2019.

Figure 6.13. Constitutive model for concrete (Yamamoto et al., 2008)

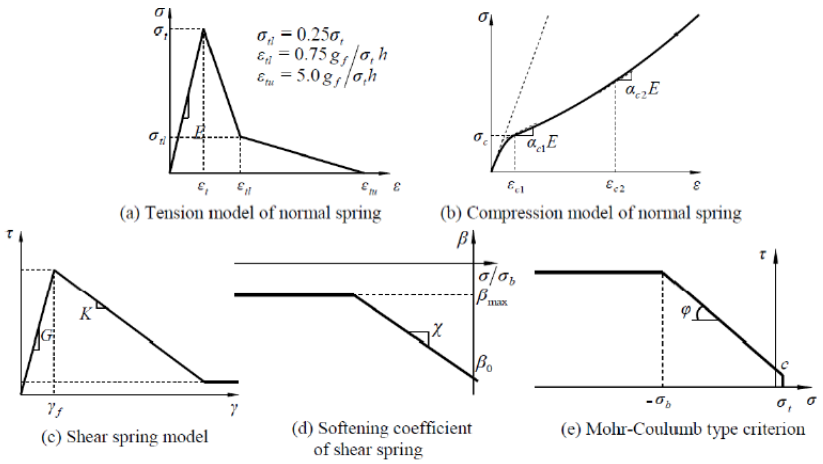

Source: NEA, 2019.

Figure 6.14 (left) shows the typical hysteresis loop of the normal spring under reversed cyclic loading. The number on the loops shows how the loading was applied. The stiffness of the unloading is initial elastic modulus *E*. In addition, after the stress reaches zero on the unloading path, the stress remains zero until the strain reaches zero. The reloading paths pass toward the start point of the unloading. Figure 6.14 (right) shows the typical hysteresis loop of the shear spring. The stiffness of the unloading and reloading is initial elastic modulus *G*. In addition, after the stress reaches zero on the unloading path, the stress keeps at zero until the strain reaches the residual strain of the opposite sign.

Figure 6.14. Hysteresis of stress-strain relations for constitutive sprigs for concrete: normal (left) and shear (right) spring

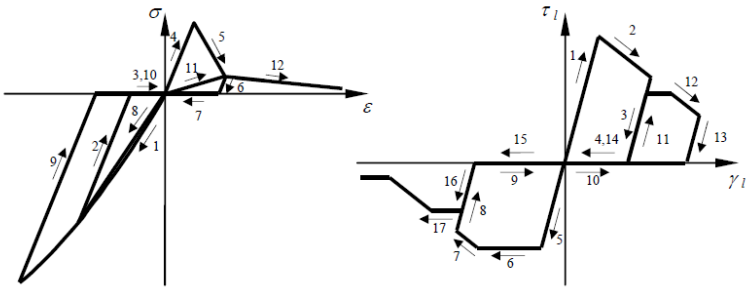

Source: NEA, 2019.

The reinforcing bar is modelled as a series of regular beam elements (Figure 6.15) that can be freely located within the structure, regardless of the concrete mesh design (Bolander and Saito, 1998). Three translational and three rotational degrees of freedom are defined at each beam node. The reinforcing bar is attached to the concrete particles by means of zero-size link elements that provide a load-transfer mechanism between the beam node and the concrete particles. For the reinforcing bar, the bilinear kinematic hardening model is applied. The hardening coefficient is 1/100. Crack development is strongly affected by the bond interaction between concrete and reinforcing bar. The bond stress-slip relation is provided in the spring parallel to the reinforcement of the linked element.

Figure 6.15. Arrangement of beam and link elements (left) and bond stress-slip model (right)

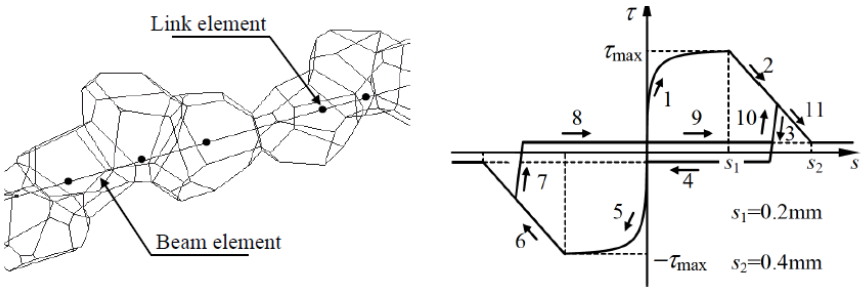

Source: NEA, 2019.

The proposed ASR model is composed of a chemical model and expansion model. In the chemical model, the amount of ASR gel (*Vgel*) is estimated. The input parameters of the model are aggregate size, reactive aggregate rate and alkali amount. In addition, the model considers the reaction rate of aggregate as described later. In the expansion model, expansion strain is estimated. The expansion strain is described by *Vgel* and expansion reduction effect due to absorption area surrounding each aggregate and expansion crack itself.

In order to discuss the reproducibility of the phenomenon that the expansion amount of ASR remarkably decreases under confinement pressure, three different models are prepared as follows:

1. Isotropic expansion model: All elements can generate expansion corresponding to the expansion model isotropically. The expansion pressure of each element is averaged by total expansion due to the reactive aggregate amount.
2. Stress-dependent expansion model: In this model, the expansion strain ε_{ASR} is also introduced to the normal springs of all RBSM elements. However, for the normal spring in the compression stress state, the expansion strain ε_{ASR} is multiplied by a reduction coefficient.
3. Distributed expansion model: The expansion strain ε_{ASR} is only introduced to the normal springs of the reactive elements, which are randomly selected. The reactive elements are selected by using the minimum distance between reactive elements R (mm) in order to arrange the elements at a constant interval.

Analysis results

The load–displacement curves of the test and numerical results of the regular specimens are compared in Figure 6.17. In the figure, the results of both the monotonic and the cyclic loading simulations results are shown. In addition, the force-displacement curves obtained by the test are shown as the envelope curve of the hysteresis loop. The simulation results show that in the case of cyclic loading the load capacity and the ductility are slightly lower than in the case of monotonic loading. Figure 6.17 (left) shows the results of ASR-affected cases. The simulation results show that the load capacity decreases due to alkali aggregate reaction. In the test result, the alkali aggregate reaction slightly increases the capacity and significantly decreases ductility.

Figure 6.16. Force-displacement curves for regular and ASR specimens, tests and simulations

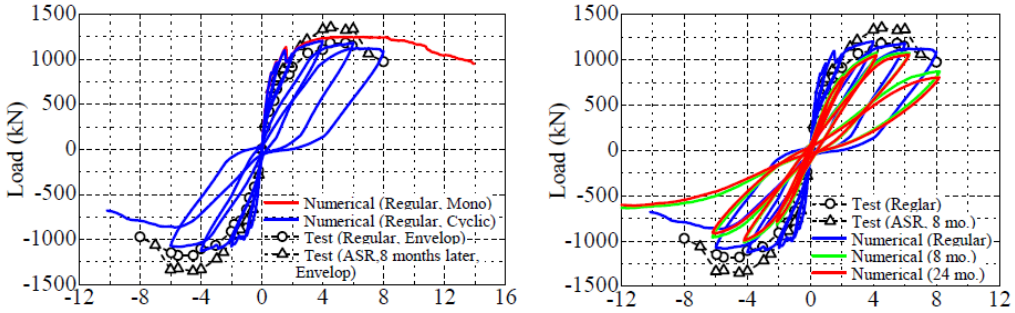

Source: NEA, 2019.

Figure 6.17. Comparison of the failure modes in simulations and test for regular wall (left) and ASR wall (right)

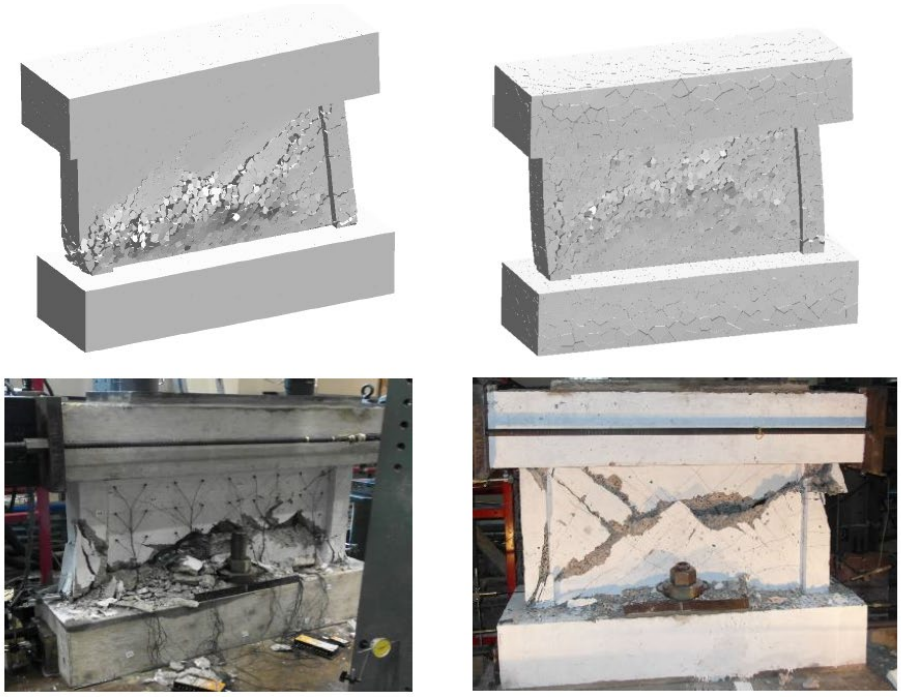

Source: University of Toronto, 2022.

Figure 6.17 shows good agreement between the simulations and the tests results in terms of predicating the failure modes and the difference in failure modes for regular concrete and the concrete with alkali aggregate reaction.

6.7 Scanscot presentation

Modelling

The software used in the analysis is ABAQUS/Explicit. The model was built using 3D solid elements and reinforcement was modelled using discrete bars with no bond slip. The lower and upper beams were modelled as elastic. The concrete constitutive model was concrete

damage plasticity model form ABAQUS. The alkali aggregate reaction was modelled using a simplified engineering approach as isotropic (thermal) expansion. In Phase II the model underestimated the capacity of both the regular and reactive wall. The failure mode was ductile failure mode. The new feature used in Phase III was a bond interaction between the reinforcement and the concrete. The analysis was done for monotonic loading only.

Figure 6.18. Influence of bond slip for regular wall without (left) and with (right) bond slip

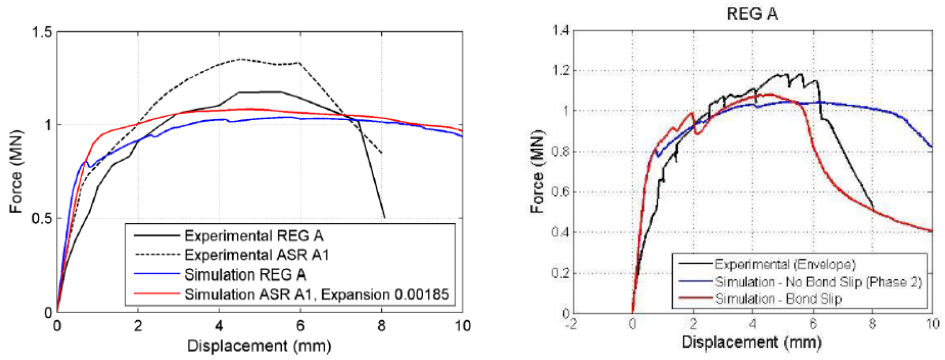

Source: NEA, 2019.

Figure 6.19. Bond slip model

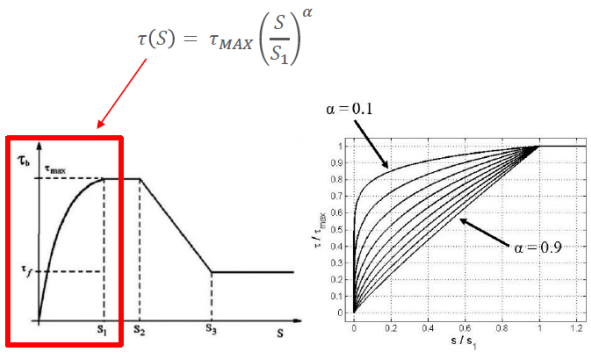

Source: NEA, 2019.

Sensitivity studies

Sensitivity studies were performed varying the parameters in the bond slip model and it was found that the results in terms of ultimate capacity, ductily and crack distribution are very sensitive to small variations in model parameters.

Figure 6.20. Results of sensitivity studies for the wall with alkali aggregate reaction ASR A1

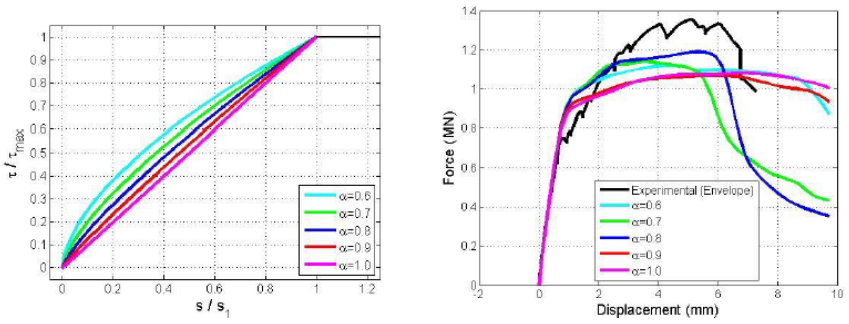

Source: NEA, 2019.

6.8 UC Davis report

Software

The software used was MS ESSI Simulator (Modelling and Simulation of Earthquakes, and/or Soils, and/or Structures and their Interaction), which is also known as the Real ESSI Simulator. MS ESSI Simulator is a software, hardware and documentation system for high fidelity, high performance, time domain, non-linear/inelastic, deterministic or probabilistic, 3D, finite element modelling and simulation of (a) statics and dynamics of soil, (b) statics and dynamics of rock, (c) statics and dynamics of structures, (d) statics of soil-structure systems, and (e) dynamics of earthquake-soil-structure system interaction.

Modelling

Beam slabs and steel plates are modelled using a 27-node brick element, while steel bolt is represented as a single truss element. The shear wall is modelled using non-linear layered plane stress elements. For the web part of the wall, the elements have a horizontal rebar layer, a vertical rebar layer, and an unconfined concrete layer. For the boundary elements (columns) of the shear wall, the elements have an additional layer of confined concrete. It is emphasised that the main wall is really made from unconfined concrete, and the only actually confined concrete is within concrete boundary elements. The bottom of the model is restrained in all directions, while the lateral sides of the bottom beam slab are restrained in direction of imposed motion. Since the shear wall consists of 2D plane stress elements, the out-of-plane displacement is also precluded. The sides of the top beam slab are also restrained to have the same displacement, which is important to represent the boundary conditions of the physical experiment. The initial model included inelastic contact elements (stick-slip and gap open and close) at the bottom boundary. However, it was concluded that there will be no slip and there is no gap opening, so these elements were removed to speed up computations.

Figure 6.21. US Davis FE model with boundary conditions

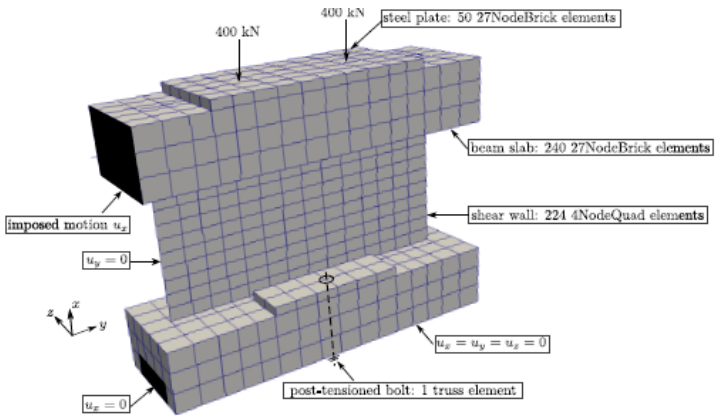

Source: NEA, 2019.

Concrete constitutive law

The concrete material model used in this study was developed by Faria et al. (1998). The model features are:

- distinct stress-strain envelopes obtained under compression or under tension;
- stiffness recovery after loading reversal;
- higher concrete strength under 2D or 3D compression test, compared to 1D loading;
- plastic deformations discernible after some compressive stress limit is reached.

Analysis results

The ESSI simulation curves show good agreement with experimental results. The differences in the envelopes of the cyclic loading curves, between the numerical and experimental results, are within 10%. The shear strengths and failure loads/displacements given by ESSI simulations match well with the values determined by physical experiments for regular walls (Figure 6.22). Note that this particular case with ASR concrete (ASR A1) has a much larger unloading-reloading cyclic area, which means that ASR concrete has the capability of dissipating more input energy (Figure 6.23). It is important to note that this conclusion does not hold for other ASR concrete walls that were tested (ASR B1 and ASR B2).

Figure 6.22. Hysteresis loops for REG A (a) and REG B (b) walls

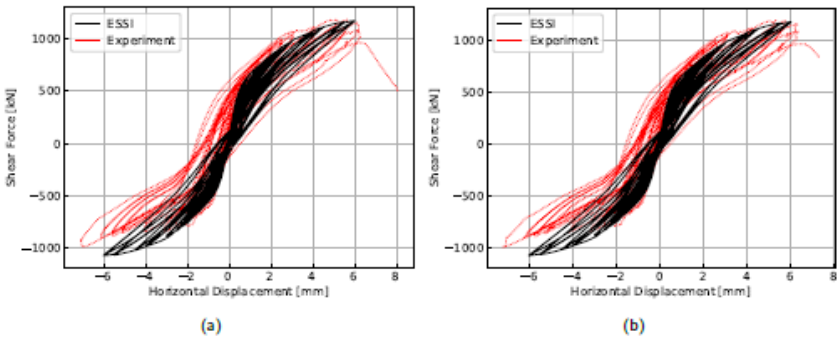

Source: NEA, 2019.

This might indicate that for some structures with the ASR concrete, it is possible to dissipate more seismic energy if the structure is under earthquake cyclic loading. On the other hand, for some other structure with the ASR concrete, such conclusion might not hold as other test data suggests reduction of seismic energy dissipation capacity. This leads to the conclusion that variability of ASR concrete quality and material behaviour can be significant.

Figure 6.23. Hysteresis loops for ASR A1 wall

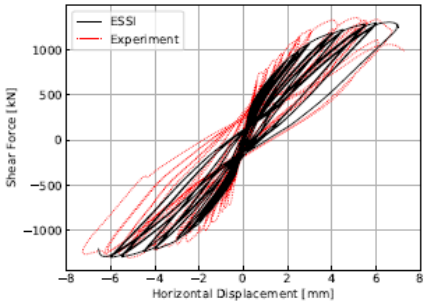

Source: NEA, 2019.

7. Discussion

The CNSC and UC-Davis analyses are two simulations that captured well some aspects of the test results and the wall behaviour. The hysteresis loop shapes for the regular walls and the wall with ASR tested for the shorter ageing period were captured well by the UC-Davis analyses. Unfortunately, the UC-Davis analyses did not include the two tests with advanced alkali aggregate reaction. The CNSC study predicted well the loss of ductility and energy absorption. However, it is not clear why those two sets of simulations were better in those predictions. The CNSC used a simple approach for modelling concrete expansion due to alkali aggregate reaction using thermal expansion. The concrete model and its post-peak behaviour under compression could be a governing parameter for modelling loss of ductility as shown in studies performed by the US NRC and the University of Toronto.

One of the most important results of the University of Toronto testing campaign on shear walls is the loss of ductility of the tested walls with alkali aggregate reaction as compared to the walls with regular concrete.

Figure 7.1. Force-displacement backbone for REG B, ASR B1 and ASR B2 walls

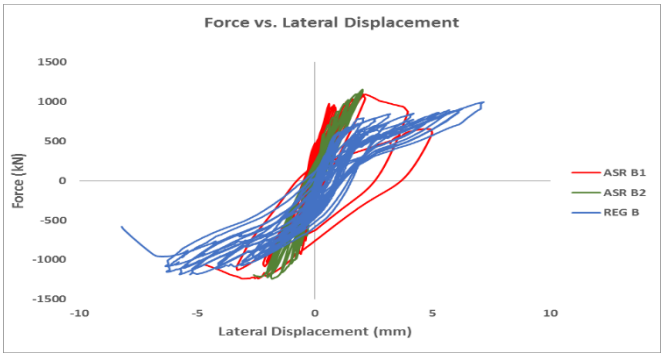

Source: NEA, 2019.

Figure 7.1 shows significant loss of ductility and energy absorption (narrow hysteresis loops) for the ASR wall compared to the regular wall. Based on the results of ASCET Phase II and ASCET Phase III benchmarks, this loss of ductility is difficult to simulate. Although the seismic design of nuclear facilities is based on essential elastic behaviour and the capacity of concrete structures, significant loss of ductility should be taken into account in the design and especially in the seismic assessment of existing structures with concrete degradation mechanisms.

The ASCE standard 43-05 provides the criteria for the design of nuclear facilities. Allowable drift limits are provided as a function of limit state and structural systems. The criteria provided below are for structural shear walls. There are four limit state (LS) criteria for four levels of seismic criteria in terms of structural drift, from LS-A (conventional structures) to LS-D (nuclear power plants).

Figure 7.2 and Figure 7.3 provide force-displacement curves for the regular walls and walls with alkali aggregate reaction with the design criteria in terms of allowable drifts. The limits are calculated as a function of the drift and plotted on figures. For shear controlled walls,

ASCE 43-05 (Seismic Design Criteria for Structures, Systems and Components in Nuclear Facilities) provides for:

- LS-A and LS-B (conventional structures) 0.75% and 0.6%, respectively, and
- LS-C and LS-D (nuclear structures) 0.4%.

In general, assessments of existing structures adopt less stringent acceptance criteria than for the design of new builds. For shear controlled walls of existing conventional structures, ASCE 41-06 (Seismic Rehabilitation of Existing Buildings) provides for conventional longitudinal reinforcement with nonconforming transverse reinforcement: LS (Life Safety) 0.8% and CP (collapse prevention) 1%. The test campaign performed at the University of Toronto does not confirm this practice. It means that the acceptance criteria for the assessment of nuclear facilities with alkali aggregate reaction, or any other concrete degradation mechanism resulting in concrete swelling, should be more stringent than for the design of new facilities.

Figure 7.2. Force-displacement backbone curve REG A wall

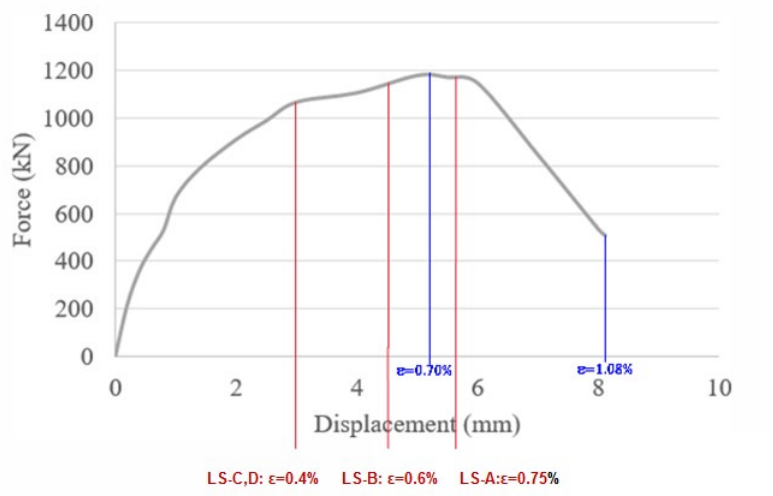

Source: NEA, 2019.

Figure 7.3. Force-displacement backbone curve REG B wall

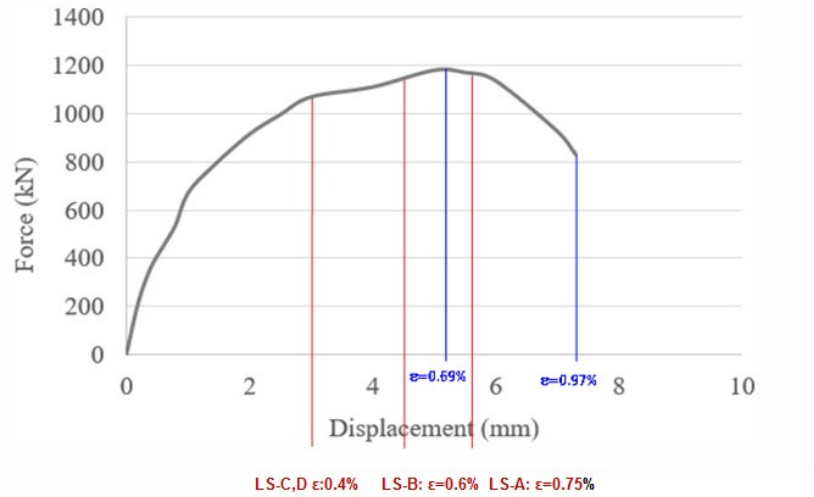

Source: NEA, 2019.

Figure 7.4. Force-displacement backbone curve ASR B1 wall

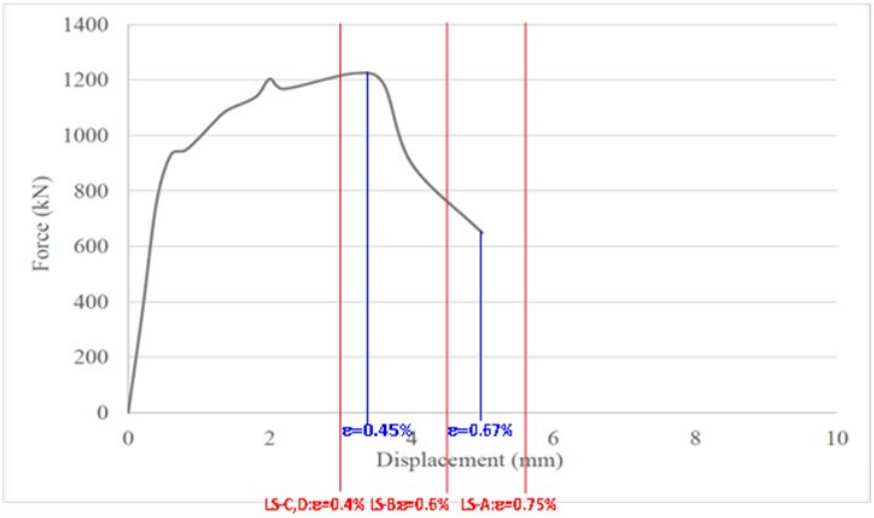

Source: NEA, 2019.

Figure 7.5. Force-displacement backbone curve ASRB2 wall

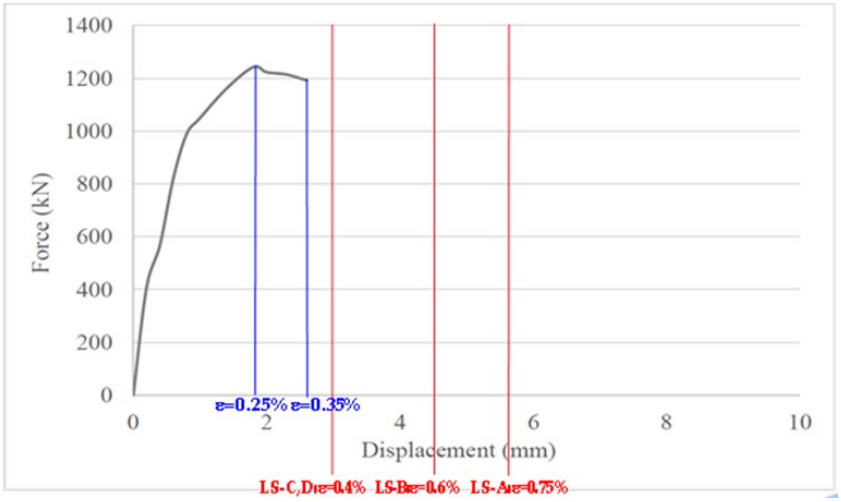

Source: NEA, 2019.

The provided design and assessment criteria are fully applicable to walls with regular concrete, as can be seen in Figure 6.22 and Figure 7.2. However, the criteria cannot be applied to the walls with alkali aggregate reaction. Despite the same, even higher, ultimate capacity, the structural resistance under cyclic loading can be significantly lower. This lower resistance is difficult to simulate numerically and the acceptance criteria are not established. Moreover, reduced energy absorption, which can be seen in very narrow hysteresis loops, shows the reduction in structural damping. It means that the structural damping of 7%, which is used for design, or 10%, used for the assessment of existing facilities, is too high for concrete structures with alkali aggregate reaction. The reduced structural damping results in higher seismic demand. It is not possible to define structural

damping based on quasi static tests, as performed at the University of Toronto under the CNSC research program. It is necessary to conduct dynamic tests. Based on quasi static tests, it is possible to see that there will be a reduction in structural damping but it is not possible to quantify this reduction.

The assessment of facilities with alkali aggregate reaction (or any other concrete degradation resulting is swelling of concrete) requires special attention as both the structural demand and structural capacity are modified compared to the structures constructed with regular concrete. Maximum shear capacity is unchanged, even higher, than in regular walls. However, for repeated cycling loading for structures with AAR, the number of cycles and duration of the loading becomes the main loading parameter and not the maximum shear force.

8. Conclusions

Five walls were tested at the University of Toronto as described in Chapter 1. The main conclusions of the test campaign are:

- The walls with alkali aggregate reaction have the same or even slightly higher ultimate shear capacity compared with the walls made of regular concrete, despite reduced compressive and tensile concrete strengths. Therefore, the code equations for the design of concrete elements based on concrete compressive strength are not applicable.
- The behaviour of the regular walls did not change significantly with time.
- The behaviour of the walls with alkali aggregate reaction experience with time significant loss of ductility and energy absorption, and the hysteresis loops become very narrow.

Eight comprehensive studies were set up with teams using different approaches and different software.

The recommendations of Phase II workshop were issued and additional test data provided by the University of Toronto were used. Almost all participants, independently of the software used, calculated to peak strength of the walls' capacity a 10% difference in the measured values. However, similarly to the Phase II benchmark, the displacements and the shape of hysteresis loops were more difficult to simulate.

A number of sensitivity studies were performed in Phase III in order to determine governing parameters. Despite the recommendations of Phase II that boundary conditions should have a significant effect, the sensitivity studies performed by the majority of participants in Phase III concluded that it was not the case. The majority of participants adopted a fixed base model to reduce computing time without significant impact on the results. Displacements, deformations, failure modes and crack patterns were addressed in detail in the Phase III benchmark. Each participant provided global wall response in terms of force-displacement curves as well as crack patterns and failure modes.

The US NRC performed a limited sensitivity study with a range of parameter values beyond the values of the baseline specimen with parameters provided by the University of Toronto. The parameters were: a) aggregate size, b) unconfined concrete expansion, c) concrete behaviour under compression (concrete model combination), and d) concrete expansion models. In all cases the failure mode changed from shear failure mode to sliding at the contact between the wall and the lower beam. High sensitivity to small input parameter modifications was recorded. For example, the change of unconfined expansion due to the ASR from 0.32% to 0.35%, or the change of aggregate size from 20 mm to 15 mm, produce a change in the failure mode from shear to sliding. The wall capacity is unchanged by the change in failure mode. However, the displacements are much lower for the sliding mode of rupture, but the shape hysteresis loops are not very different. The difference is that the failure mode happens after a smaller number of loading cycles for sliding than for shear failure mode (lower displacements).

Scanscot performed a sensitivity study related to the bond between the reinforcement and surrounding concrete. The study concluded high sensitivity, of both failure mode and ductility, to bond model parameters.

The EDF study put an emphasis on concrete crack re-closures parameter (REF). The sensitivity study showed the influence of this parameter on the ductility and overall failure energy.

Nagoya University used the discrete element method RBSM that can quantitatively reproduce not only the detailed cracking information but also the compressive softening and localised behaviour (including the quantitative evaluation of the localised volume) with/without lateral constraint. This was the only discrete element method used in this benchmark. The failure modes were successfully modelled. However, the capacity of walls with alkali aggregate reaction was lower than regular walls, which is not in accordance with test results. The simulation did not reproduce the energy absorption reaction in hysteresis loops either. On the other hand, the loss of ductility due to alkali aggregate reaction was reproduced.

The NRA performed a series of sensitivity studies, including variation of the concrete compressive strength due to alkali aggregate reaction. With the lower bound of the compressive strength due to the alkali aggregate reaction, the peak shear force was achieved with the displacement still well above the displacements in the tests.

The sensitivity studies performed by the University of Toronto concluded that three factors had a notable effect on the computed response: the boundary conditions, strength enhancement due to confinement and concrete compression response. However, the sensitivity studies have not shown the main factor for reduction of ductility and energy absorption.

The CNSC predicted successfully the loss of ductility and energy absorption in walls with alkali aggregate reaction using the input data provided by the University of Toronto. The concrete expansion due to alkali aggregate reaction was approximated with isotropic thermal expansion using the Eurocode2 concrete model implemented in LS-DYNA software.

UC-Davis used the MS ESSI Simulator, developed at UC Davis. The UC-Davis analysis, which used the Faria et al. concrete model, predicted within a 10% range the hysteretic behaviour of regular walls and ASR A1 wall with alkali aggregate reaction. The walls with advanced alkali aggregate reaction, ASR B1 and ASR B2, were not modelled. The question remains whether the model could simulate the modification in wall behaviour, loss of ductility and energy absorption with advanced alkali aggregate reaction.

The loss of ductility and energy absorption (hysteretic damping) of walls with ASR concrete, compared to walls regular concrete, is an important finding of the test campaign performed at the University of Toronto. The ASCET program found that the losses of ductility and energy absorption are difficult to model. Special attention should be paid to the assessment of concrete structures with ASR (or any other degradation mechanism resulting in concrete swelling), in particular the simulation of those phenomena and corresponding acceptance criteria.

9. Recommendations

Based on the conclusions of the testing campaign on shear walls performed at the University of Toronto under the CNSC research programme and the ASCET Phase III numerical benchmarks:

- There is a need to provide acceptance criteria for the design and assessment of concrete structures with alkali aggregate reaction (or any other degradation mechanism resulting in concrete swelling).
- The code equations related to the design capacity of concrete elements which are based on concrete compressive strength are not applicable. Moreover, the capacity is not directly correlated to the allowable displacements and drifts, as in design standards. Therefore, there is a need to provide separate, uncorrelated sets of acceptance criteria in terms of capacity and deformations.
- The deformation limits are governing, and, that should be taken into account in the assessment phase.
- New damping values for reinforced concrete elements with alkali aggregates reaction (or any other concrete degradation resulting in concrete swelling) should be provided. The values in current design and assessment standards are high compared to the tests and results in underestimating structural demand. Dynamic tests are needed in order to quantify the structural damping.
- Special attention should be paid to repeated cyclic loading, such as seismic loading, as the reduced ductility and structural damping will reduce the structural capacity and increase structural demand.

All participants captured well the peak strength capacity of walls with alkali aggregate reaction. Only a few simulations could capture the reduction of the ductility and energy absorption of the tested walls with the advanced ASR, and the shape of hysteresis loops. However, the reasons for these successful simulations are unclear.

The concrete constitutive model and its post-peak behaviour could be the reason. It is necessary to vary the concrete model in these simulations and to perform sensitivity studies in order to determine the governing parameters leading to the significant loss of ductility.

The results are sensitive to small variations in input parameters, resulting in different failure modes and/or modification in structural ductility (cliff-edge effect). The materials and their characteristics should be carefully defined based on material specifications and tests results.

References

Bolander, J.E. and S. Saito (1998), "Fracture analyses using spring networks with random geometry", *Engineering Fracture Mechanics*, Vol. 61, pp. 569-591, doi.org/10.1016/S0013-7944(98)00069-1.

Charlwood, R.G., S.V. Solymar and D. D. Curtis (1992), "A review of alkali aggregate reactions in hydroelectric plants and dams", in *Proceedings of the International Conference of Alkali-Aggregate Reactions in Hydroelectric Plants and Dams*, Fredericton, Canada, pages 129-135.

Faria, R., J. Oliver and M. Cervera (1998), "A strain-based plastic viscous-damage model for massive concrete structures", *International Journal for Solids and Structures*, Vol. 35, No. 14, pp. 1533-1558, doi.org/10.1016/S0020-7683(97)00119-4.

Gautam, B.P., D.K. Panesar, S.A. Sheikh, F.J. Vecchio and N. Orbovic (2015), "Alkali aggregate reaction in nuclear concrete structures: Part 2: Material Aspects", SMiRT-23, Manchester, United Kingdom, 10-14 August.

Gocevski, V. (2016), "Constitutive Framework for Modeling of AAR in Concrete/ Reinforced Concrete", ASR management of important and long-life structures, dams, nuclear power relating facilities, and radioactive wastes disposal, Appendix of the Extended Abstract prepared for the work shop held on 29 March 2016, Tokyo, Japan.

Hoshikuma, J., K. Kawashima, K. Nagaya and A.W. Taylor (1997), "Stress-strain model for confined reinforced concrete in bridge piers", *J. of Structural Engineering, American Society of Civil Engineers* (ASCE), Vol. 123, No. 5, May, 1997, doi.org/10.1061/(ASCE)0733-9445(1997)123:5(624).

Kawai, T. (1978), "New discrete models and their application to seismic response analysis of structures", *Nuclear Engineering and Design*, 48, pp.207-229.

Maekawa, K., Fukuura N., An, X.(2001),"2D and 3D Multi-directional Cracked Concrete Model under Reversed Cyclic Stresses", Modeling of Inelastic Behavior of RC Structures under Seismic Loads, ASCE, pp56-78

Miyahara, T., Kawakami, T. and Maekawa, K. (1987), "Nonlinear behavior of cracked rreinforced concrete plate element under uniaxial compression", *Journal of JSCE*, 1987(378), 249-258. (in Japanese)

Montoya, E. (2003), "Behaviour and Analysis of Confined Concrete", PhD Thesis. Department of Civil Engineering, University of Toronto, pp 321.

NEA (2017), "Final Report on the Phase 1 of the Assessment of Structures Subjected to Concrete Pathologies (ASCET)", OECD Publishing, Paris, www.oecd-nea.org/jcms/pl_19738.

Popovics, S. (1973), "A Numerical Approach to the Complete Stress-Strain Curve of Concrete", *Cement and Concrete Research*, Vol. 3, No.5, pp. 583-599, doi.org/10.1016/0008-8846(73)90096-3. (Modified for high-strength concrete in: Collins M P, Porasz A., "Shear design for high-strength concrete", Comité Euro-International du Béton, CEB Bulletin d'Information, 1989, 193: 77–83).

Sellier, A., E. Bourdarot, S. Multon, M. Cyr and E. Grimal, E. (2009), “Combination of Structural Monitoring and Laboratory Tests for Assessment of Alkali-Aggregate Reaction Swelling: Application to Gate Structure Dam”, *ACI Materials Journal*, Vol. 106, No. 3, May-June 2009, pp. 281-290, doi.org/10.14359/56553.

Vecchio, F.J. (1992), “Finite Element Modeling of Concrete Expansion and Confinement", *ASCE Journal of Structural Engineering*, Vol. 118, No. 9, pp. 2390-2406, doi.org/10.1061/(ASCE)0733-9445(1992)118:9(2390) (as modified in: Vecchio, F.J. and Collins, M.P., 1993, "Compression Response of Cracked Reinforced Concrete", *ASCE J. of Structural Engineering*, Vol. 119, No. 12, pp. 3590-3610).

Wong, P.S., F.J. Vecchio and H. Trommels (2002), “VecTor2 and Formworks User’s Manual”, Second Edition, University of Toronto, Toronto, Canada.

Yamamoto, Y., H. Nakamura, I. Kuroda and N. Furuya (2008), “Analysis of compression failure of concrete by three-dimensional rigid body spring model”, Proceedings of Japan Society of Civil Engineers, E-64, 612-630 (in Japanese).